

produced 25.3% and 64.9% lysis of SKOV3 cells, respectively. The B1D2 x NM3E2 scFv₂ promoted cytotoxicity at concentrations as low as 100pg/ml. Thus, high affinity binding to tumor antigens increases bispecific scFv₂-mediated cytotoxicity, possibly because the slow off-rate of the higher affinity bispecific scFv₂ prolongs its cell surface retention. Additional bispecific constructs are currently being tested to further examine the role of affinity over a 10,000-fold range of K_D values.

#2993 Antibody-TNF fusion constructs targeting HER2 can overcome HER2-mediated resistance to TNF. Rosenblum, M., Parakh, C., Horn, S., and Cheung, L. *University of Texas—M.D. Anderson Cancer Center, Houston, TX 77030.*

Overexpression of the proto-oncogene HER2/NEU in breast cancer and certain other tumors appears to be a central mechanism which may be partly responsible for cellular progression of the neoplastic phenotype. Transfection studies with HER2/NEU results in reduced sensitivity to TNF's cytotoxic effects and reduced sensitivity to immune effector killing. The single-chain recombinant antibody sv23 recognizes the cell-surface domain of HER2. The cDNA for this antibody was fused to the cDNA encoding human TNF and this fusion construct was cloned into a plasmid for expression in *E. coli*. The fusion protein was expressed as insoluble inclusion bodies and renatured after solubilization in 6M guanidine and purified by ion exchange chromatography. SDS-PAGE demonstrated a single band at the expected molecular weight (43 kDa). The fusion construct was tested for TNF activity against L-929 cells and found to have TNF activity (S.A. 420 nM). The construct was also tested by ELISA for binding against SKBR-3 (HER2 positive) cells. Cytotoxicity studies against SKBR-3 cells demonstrate that the sv23/TNF fusion construct was 500 fold more active than free TNF and therefore apparently able to overcome the HER-2 mediated resistance to TNF. Further *in vitro* studies to examine the biological properties of this agent are ongoing.

#2994 Characterization of Anti-HER-2 Monoclonal Antibodies Which Inhibit the Growth of Breast Cancer Cell Lines. Ilgen, A., Ghetie, M., Shen, G., Li, J., Uhr, J. and E. Vitetta. *Cancer Immunobiology Center, UT Southwestern Medical Center.*

HER-2, or c-erbB-2, is a member of the EGF receptor family. Overexpression of the wild type HER-2 protein, as is observed on numerous carcinomas, leads to hyperactivity of the kinase and confers a significant growth advantage on cells. Numerous groups have generated monoclonal antibodies (MAbs) against HER-2 which inhibit the growth of breast cancer cell lines. Our research had three goals: to understand the mechanisms by which anti-HER-2 MAbs inhibit the growth of breast cancer cells, how the physical properties of the MAbs related to their mechanism of inhibition, and how we can optimize the anti-tumor activity of these MAbs. We generated a panel of 113 MAbs against HER-2 in this manner, 12 of which inhibited the growth of a panel of HER-2-overexpressing breast cancer cells. To understand the mechanism of inhibition of growth, we determined whether the MAbs induced cell cycle arrest and/or apoptosis in treated cells. We found that each of these 12 MAbs signaled the cells to undergo varying degrees of apoptosis and/or cell cycle arrest and that the signaling capabilities of the MAbs correlated with both the extent of overexpression of HER-2 on the breast cancer cell lines and the affinity of the MAbs. Our next step will be to determine whether MAbs and immunotoxins against different epitopes on the HER-2 molecule are able to synergistically inhibit the growth of the breast cancer cells.

#2995 Anti-metastatic therapy of MDR human lung cancer with anti-P-glycoprotein antibody and monocyte chemoattractant protein-1 gene transduction in SCID mice. Nokihara, H., Hanibuchi, M., Yanagawa, H., Shinohara, T., Fujiki, F., Nishinura, N., Parajuli, P., Tsuruo, T., and Sone, S. *Third Department of Internal Medicine, Tokushima University School of Medicine, Tokushima 770, Japan, and Institute of Molecular and Cellular Biosciences, The University of Tokyo, Tokyo 113, Japan.*

Distant metastasis is a critical problem in the therapy of human lung cancer. In this study, we investigated whether transduction of the monocyte chemoattractant protein-1 (MCP-1)-gene into multidrug-resistant (MDR) human lung cancer cells affected the inhibition of their metastases by the anti-P-glycoprotein (P-gp) monoclonal antibody MRK16. MDR human small cell lung cancer (SCLC), H69/VP cells, were transduced with human MCP-1-gene inserted into an expression vector (BCMGSNeo). MCP-1-gene transduction had no effect on the expression of P-gp, drug sensitivity to etoposide or the *in vitro* proliferation. In the metastatic model of NK-cell depleted SCID mice, the number of metastatic colonies of MCP-1-gene transduced H69/VP cells were similar to those of parent or mock-transduced cells. However, systemic treatment with MRK16 was more effective in inhibiting the metastasis of MCP-1-producing H69/VP than mock-transduced cells. These findings suggest that local production of MCP-1 in tumor site may increase the anti-P-gp antibody dependent cell-mediated cytotoxicity. This can be a useful immunological strategy to inhibit the metastasis of MDR human lung cancer cells expressing P-gp.

#2996

Alpha particle emitter therapy of micrometastases: ²¹³Bi-J591 (anti-PSMA) treatment of LNCaP spheroids. Yang, W.-H., Ballangrud, A., McDavitt, M.R., Finn, R.A., Geerlings, M., Bander, N., Scheinberg, D.A., Sgouros, G. *Memorial Sloan-Kettering Cancer Center, NY, NY 10021, Pharmacia, Inc. Wilmington, DE 19801, Cornell University Medical Center, NY, 10021.*

Multicellular spheroids were used to investigate the feasibility of eradicating micrometastases with radiolabeled antibodies. Spheroids of LNCaP (LN3) cells were exposed to 2 concentrations of bismuth-213-labeled J591 antibody (50 and 100 μ Ci) for 4 different incubation durations (15, 30, 60 min and 18 h). J591 targets an extracellular epitope of the prostate-specific membrane antigen (PSMA), emits alphas of 60 to 90 μ m range; it has a 45.6 min. half-life, 24 spheroids of 100 to 200 μ m diameter were used for each experiment. Growth curves were obtained for each spheroid up to day 70, post-incubation. ²¹³Bi-HuM195 (anti-CD33), used as a "hot" control. Spheroids exposed to 100 μ Ci ²¹³Bi-J591 for more than 15 min. did not re-grow; controls showed growth delay but re-grow after following an 18 h incubation. The growth of spheroids exposed to 50 and 100 μ Ci ²¹³Bi-J591 was arrested only after an 18 h exposure; at days 33 and 68, medium volume ratios of 400 and 7400 between hot control and specific antibody were obtained. The results demonstrate feasibility and efficacy in using antibodies labeled with alpha particle emitting radionuclides to target small clusters of tumor cells or micrometastases. The results obtained using this spheroid model may be used, in combination, with mathematical modeling to evaluate different treatment protocols against micrometastases and to optimize such a treatment approach.

#2997 A novel humanised antibody against Prostate Specific Membrane Antigen (PSMA) for *in vivo* targeting and therapy. Hamilton, A., King, S., Liu, M., Moy, P., Bander, N., and Carr, F. *Biovation Ltd, Aberdeen AB24 3RY, UK, Department of Urology, The New York Hospital-Cornell Medical Center, New York, NY 10021, Ludwig Institute for Cancer Research, New York Branch, New York, NY 10021.*

A murine monoclonal antibody (mAb), J591, is directed against the extracellular domain of PSMA, an integral membrane protein of prostate carcinoma and of tumour vascular endothelium of a wide variety of cancers, but not normal endothelium. The mAb was "humanised" by a novel method involving specific deletion of human B and T cell epitopes. To remove B cell epitopes surface exposed residues in the frameworks of the murine J591 heavy and light chain variable region (V_H and V_L) sequences were substituted by the corresponding residues from selected human germ-line V_H and V_L sequences ("surface humanisation"). For detection and elimination of T cell epitopes, a database of human MHC class II binding peptides was searched for motifs present in the substituted V_H and V_L sequences and in addition a novel computer modelling approach termed "peptide threading" was applied. Motifs, unless also present in human germ-line antibody sequences, were deleted by substituting single amino acids, preserving the CDRs. The final sequences were re-checked for new MHC class II motifs. The designed V_H and V_L regions were constructed by mutagenesis of the murine V_H and V_L. Human IgG1 or κ constant regions were added and the composite genes transfected into NS0 cells to produce complete recombinant antibodies. These antibodies bound to PSMA (on LNCaP cells) as efficiently as the original murine antibody, and are expected to have little or no immunogenicity *in man*.

#2998 Serum TA90 immune complex correlates with recurrence following adjuvant immunotherapy for regional metastatic melanoma. Hsueh, E.C., Gupta, R.K., Yee, R., Leopoldo, Z., Qi, K., and Morton, D.L. *John Wayne Cancer Institute, Santa Monica, CA 90404.*

We previously reported a significant correlation between clinical evidence of melanoma and the presence of a circulating immune complex (IC) composed of a 90-kD tumor-associated antigen (TA90) and anti-TA90 antibody. In the present study we hypothesized a correlation between TA90-IC and clinical recurrence of melanoma following lymphadenectomy and postoperative adjuvant immunotherapy. We studied 100 melanoma patients who had undergone resection of melanoma metastases and postoperative adjuvant therapy with a polyvalent melanoma cell vaccine (PMCV), and from whom serum samples had been obtained after surgical resection but prior to initiation of vaccine therapy. These serum specimens were retrieved from cryopreserved storage, coded, and tested in a blinded manner for TA90-IC. Median follow-up was 25 months (range, 18-78 months). By univariate analysis with log rank test, a positive TA90-IC level was highly correlated with recurrence. Median disease-free survival and 3-year disease-free survival rates were 8 months and 12%, respectively, for the 50 patients with a positive TA90-IC level, compared with >25 months and >53%, respectively, for the 50 patients with a negative TA90 level ($p=0.0001$). Multivariate analysis with Cox proportional hazards regression considered TA90, number of positive lymph nodes, size of involved lymph nodes, extranodal extension, and disease-free interval: TA90 positivity was the most significant independent variable correlating with disease-free survival ($p=0.0001$). These data indicate that the presence of TA90-IC in patients with no clinical evidence of melanoma postoperatively is highly correlated with subsequent disease recurrence.

Growth and Characterization of LNCaP Spheroids: A Model used to Optimize Treatment of Micrometastases with Alpha-Particle Emitter, ^{213}Bi , Labeled Antibodies

Å.M. Ballangrud¹, W-H. Yang¹, M.R. McDevitt¹, R.D. Finn¹, M. Geerlings²,
N. Bander³, D.A. Scheinberg¹ and G. Sgouros¹.

¹Memorial Sloan-Kettering Cancer Center

²Pharmactinium, Inc.

³Cornell University Medical Center

Objectives/Background

Establish a model for optimizing treatment of micrometastases.

- micrometastases are not visualized by conventional imaging
- uptake or targeting can not be assessed
- response is not easily monitored

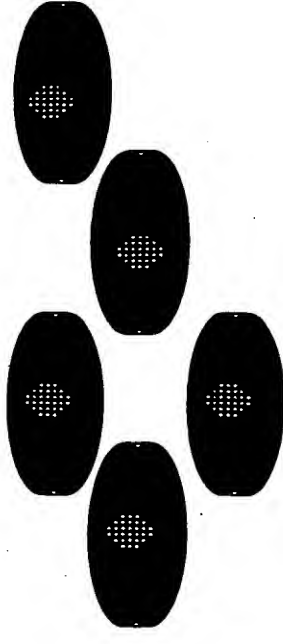
Multicellular spheroids represent an experimental model where individual parameters can be studied separately.

- provide input for model development
- geometry is ideal for determining response to short range alpha particles

LNCaP cells exhibits properties that are representative of prostate cancer, *in vivo*.

LNCaP multicellular spheroids:

experimental model for study of drug delivery and treatment response parameters to follow are growth delay and PSA production



LNCaP cells:

androgen responsive
prostatic acid phosphatase (PAP)
prostate specific antigen (PSA)
prostate specific membrane antigen (PSMA)
metastatic potential



Animal tumor models:

difficult to study micrometastatic disease



Overview

The spheroids have been characterized in terms of:

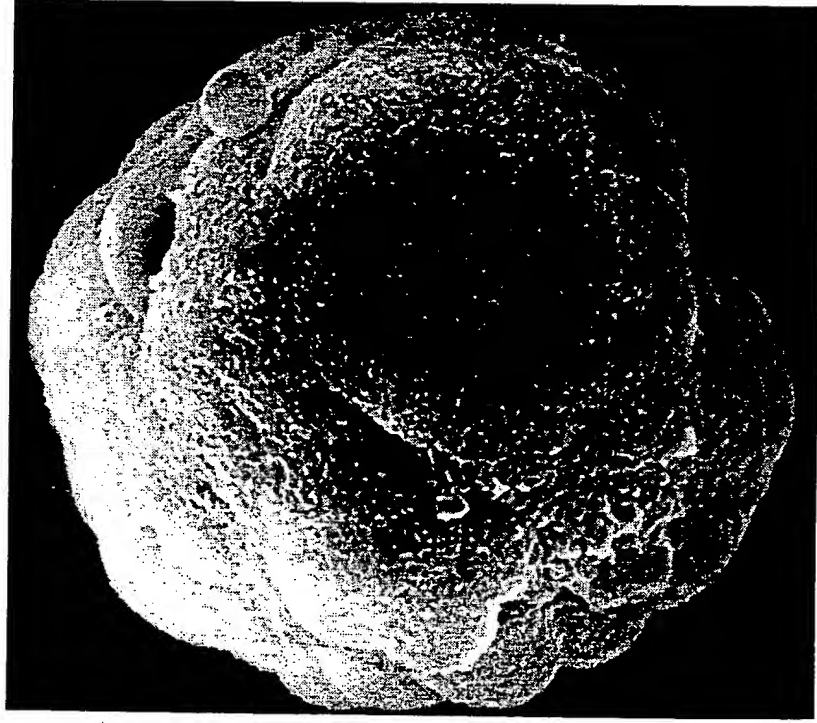
- microscopic structure
- growth kinetic parameters
- proliferating state
- PSA secretion

Preliminary results on response after alpha particle radiation

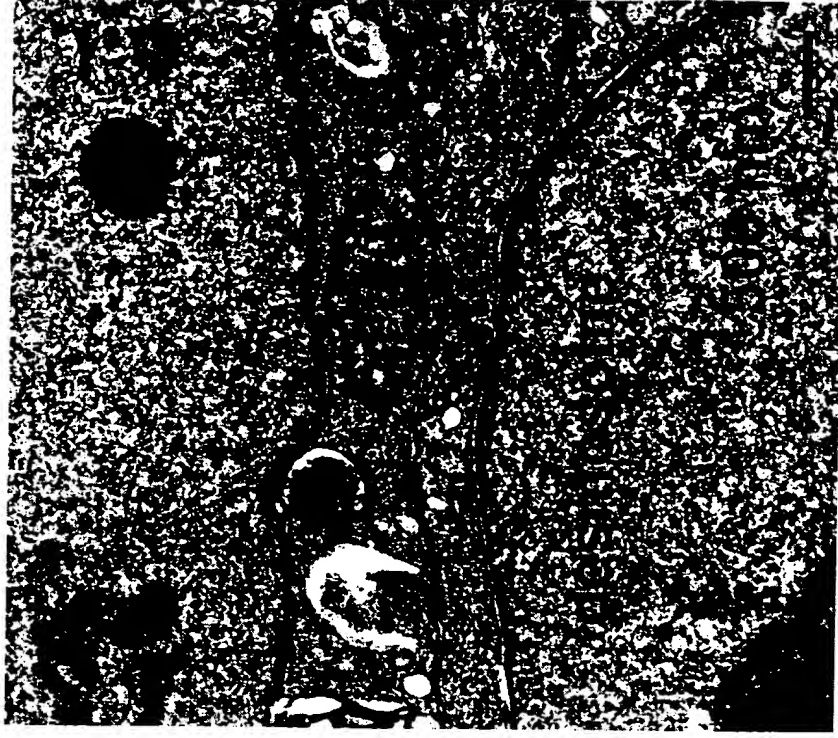
Electron Microscope Images

Scanning EM

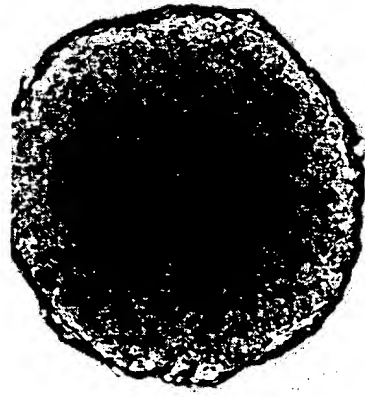
45-50 μm -diameter spheroid



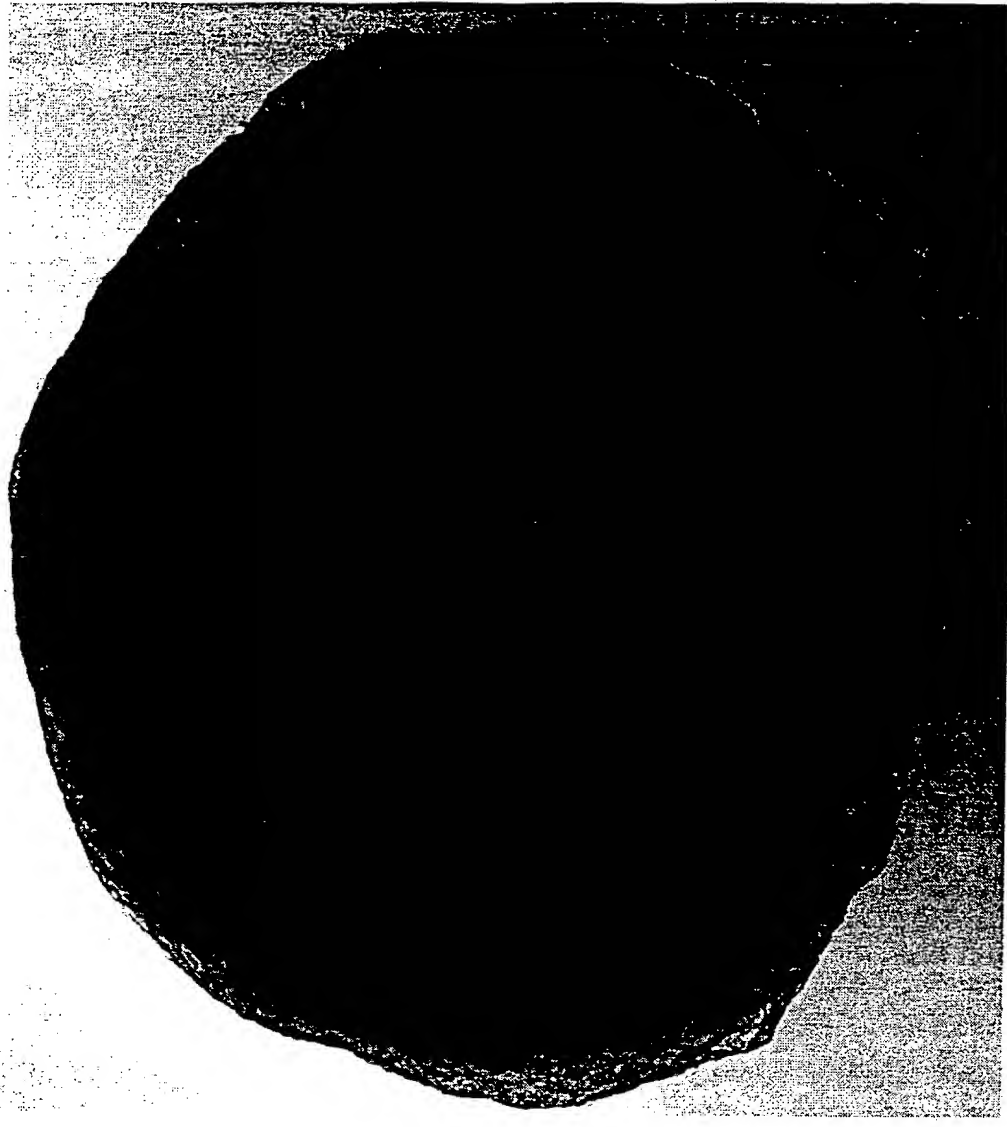
Transmission EM



Light Microscope Images

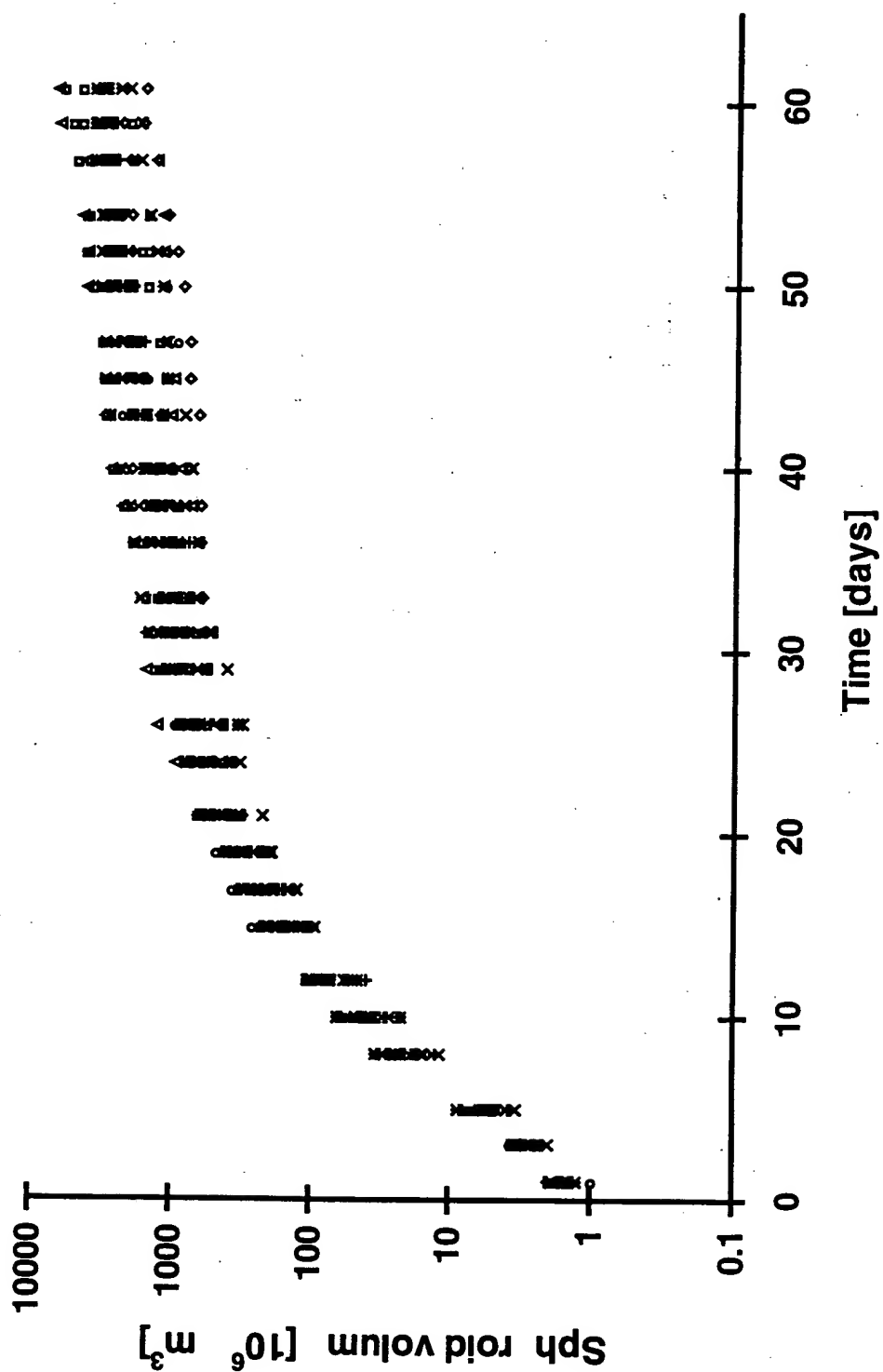


Day 12: Diameter ~ 500 μm



Day 39: Diameter ~ 1500 μm

LNCaP Spheroid Growth Curves



LNCaP Spheroid Growth Parameters

The Gompertzian equation was fitted to spheroid growth curves to determine a , b and V_0 .

$$V(t) = V_0 \exp\left(\frac{a}{b}(1 - \exp(-bt))\right)$$

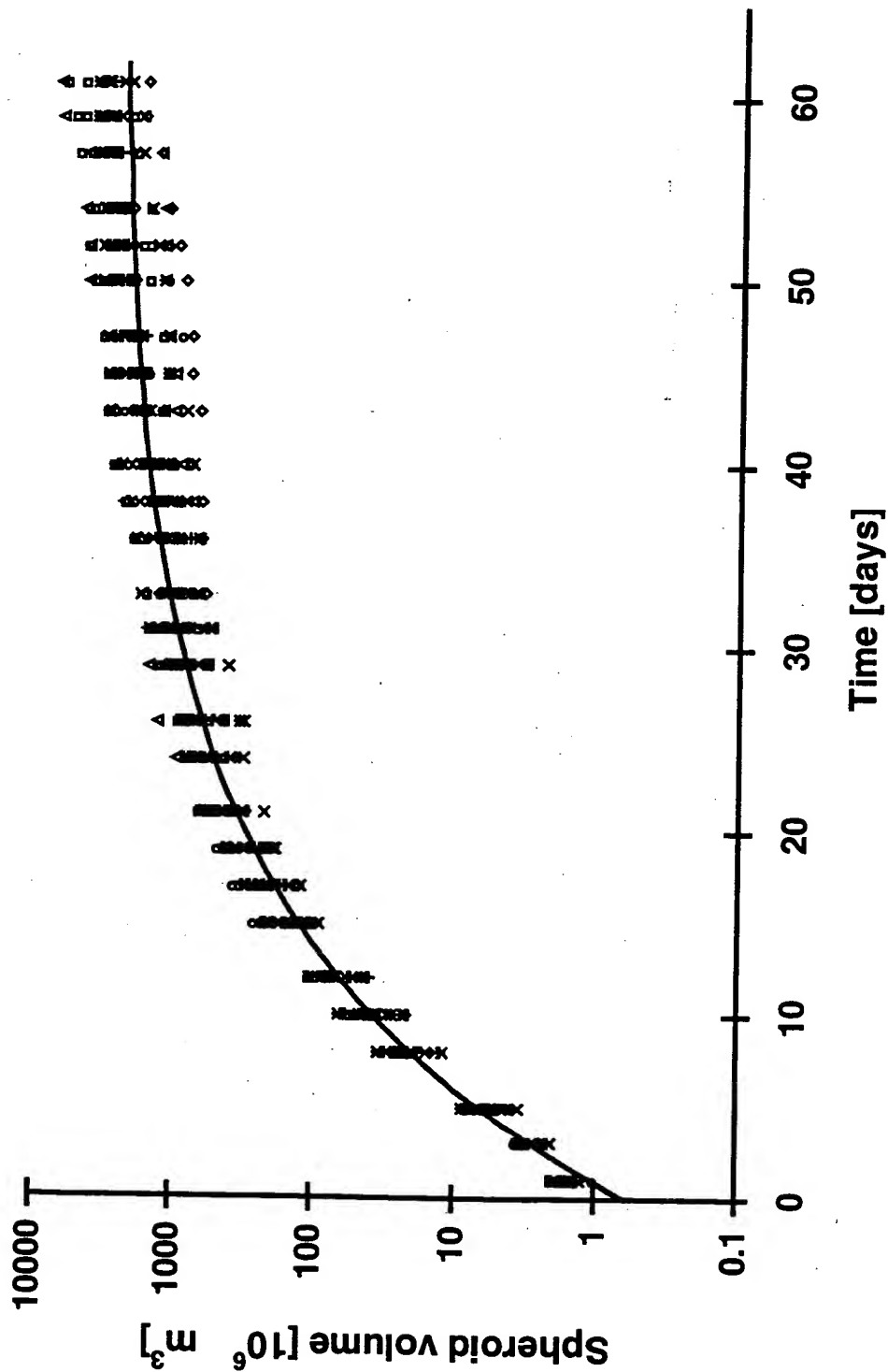
$$T = \frac{\ln 2}{a} \quad V_{\max} = V_0 \exp\left(\frac{a}{b}\right)$$

Growth parameters

LNCaP

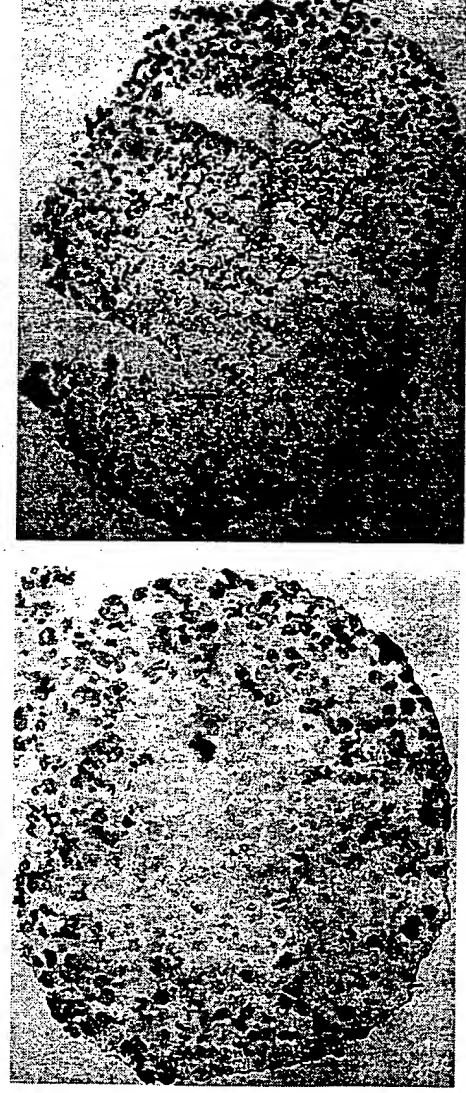
V_0 [$10^6 \mu\text{m}^3$]	0.6 ± 0.2
a [day^{-1}]	0.57 ± 0.07
b [day^{-1}]	0.068 ± 0.008
T [h]	29 ± 4
V_{\max} [$10^6 \mu\text{m}^3$]	3078 ± 1277

LNCaP Spheroid Growth Curves



Light Microscope Images of Spheroid Sections

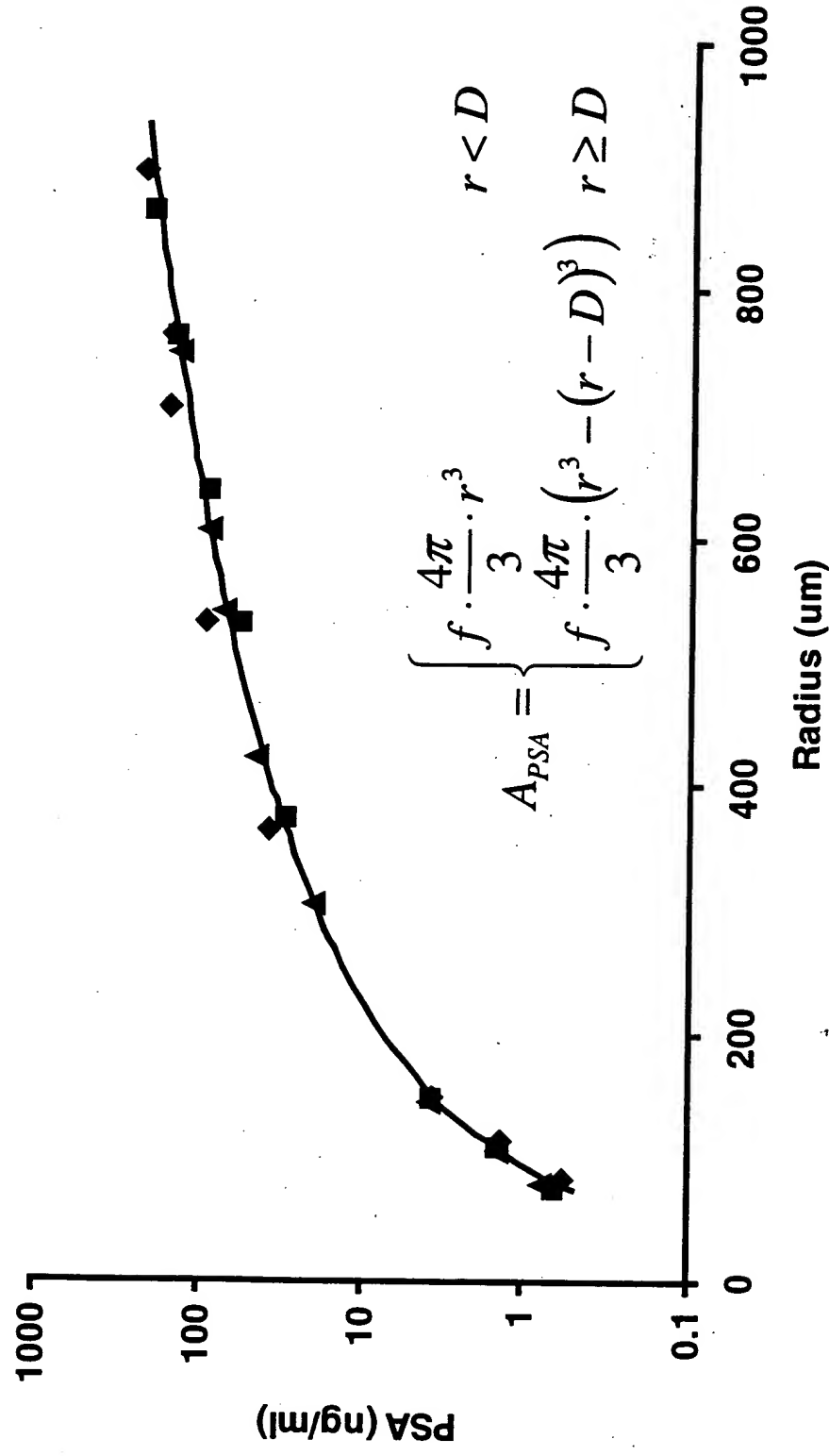
5 μm sections stained for BrdUr (brown) and counter-stained with H & E.
The shell of proliferating cells was determined to $76 \pm 13 \mu\text{m}$.



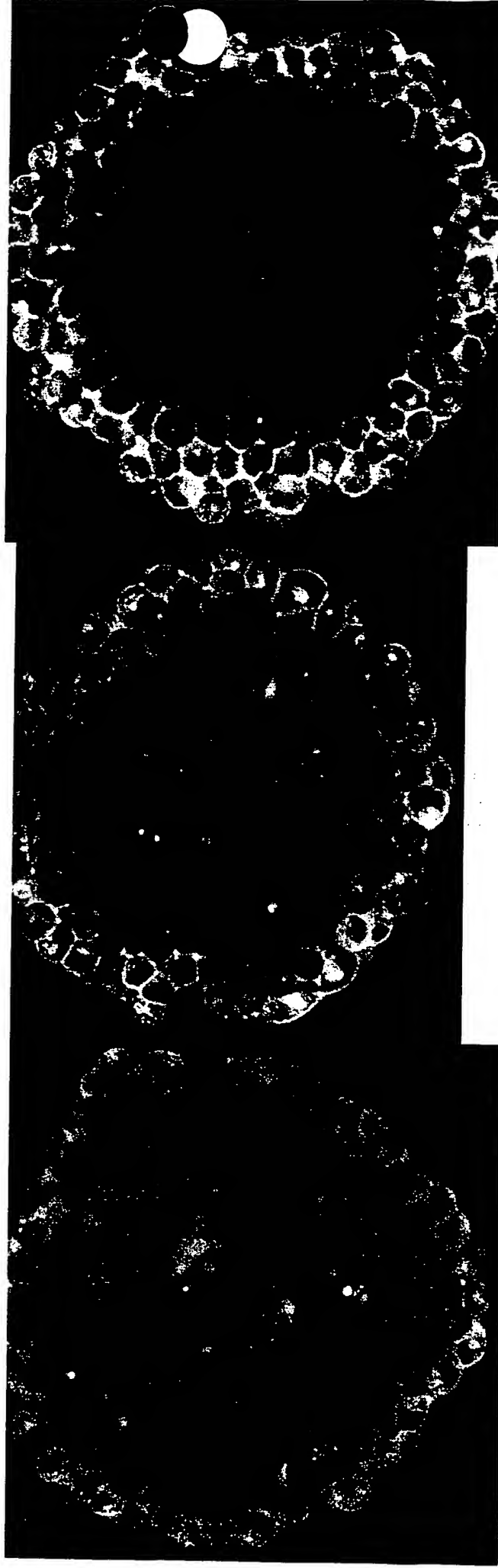
600 μm

PSA Secretion

The thickness of the shell of PSA producing cells, D , was determined to be $77 \pm 3 \mu\text{m}$ by fitting the equation to the data.



Confocal microscopy slices through the equator of LN3 spheroids following incubation with 10 $\mu\text{g}/\text{ml}$ FITC-J591.



Incubation duration (min):

15

60

120

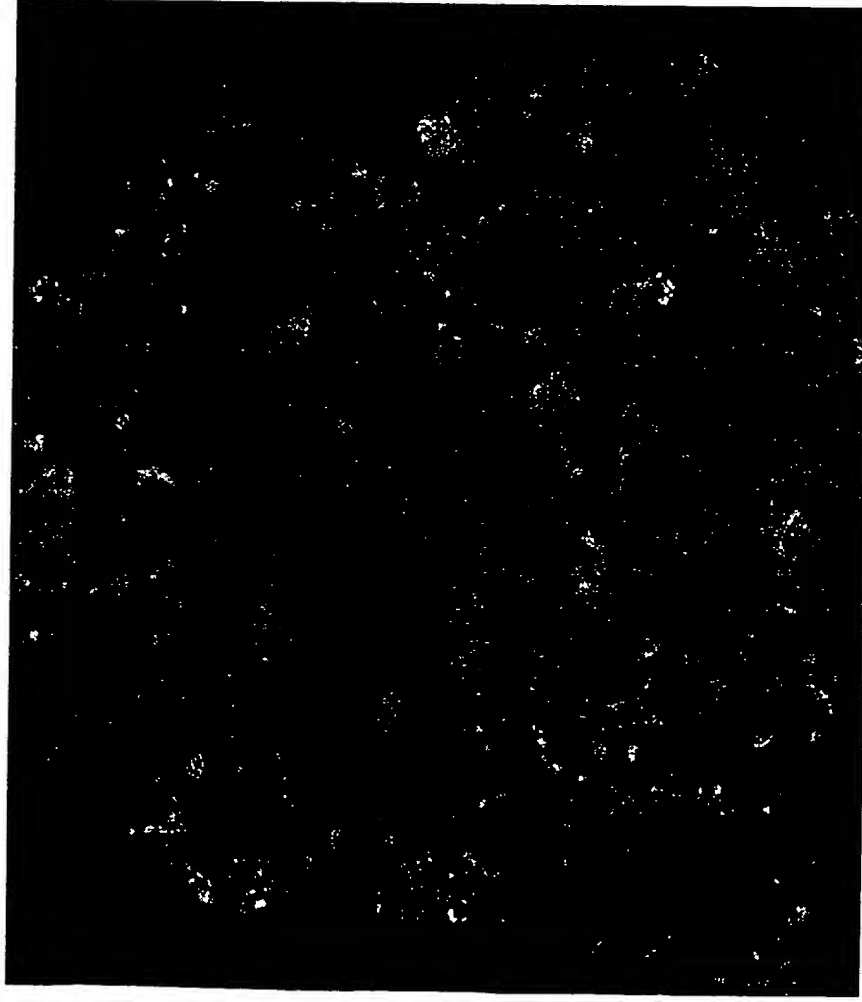
Ab penetration (cell diameters):

1

2

3

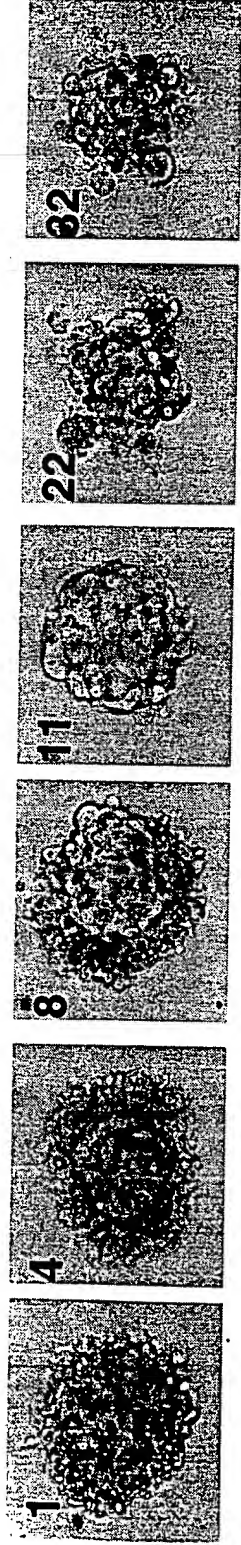
Confocal microscopy slices through the equator of 150 micron-diameter LN3 spheroids after 2 hour incubation with 10 μ g/ml FITC-HuM195 (control) or -J591 (specific).



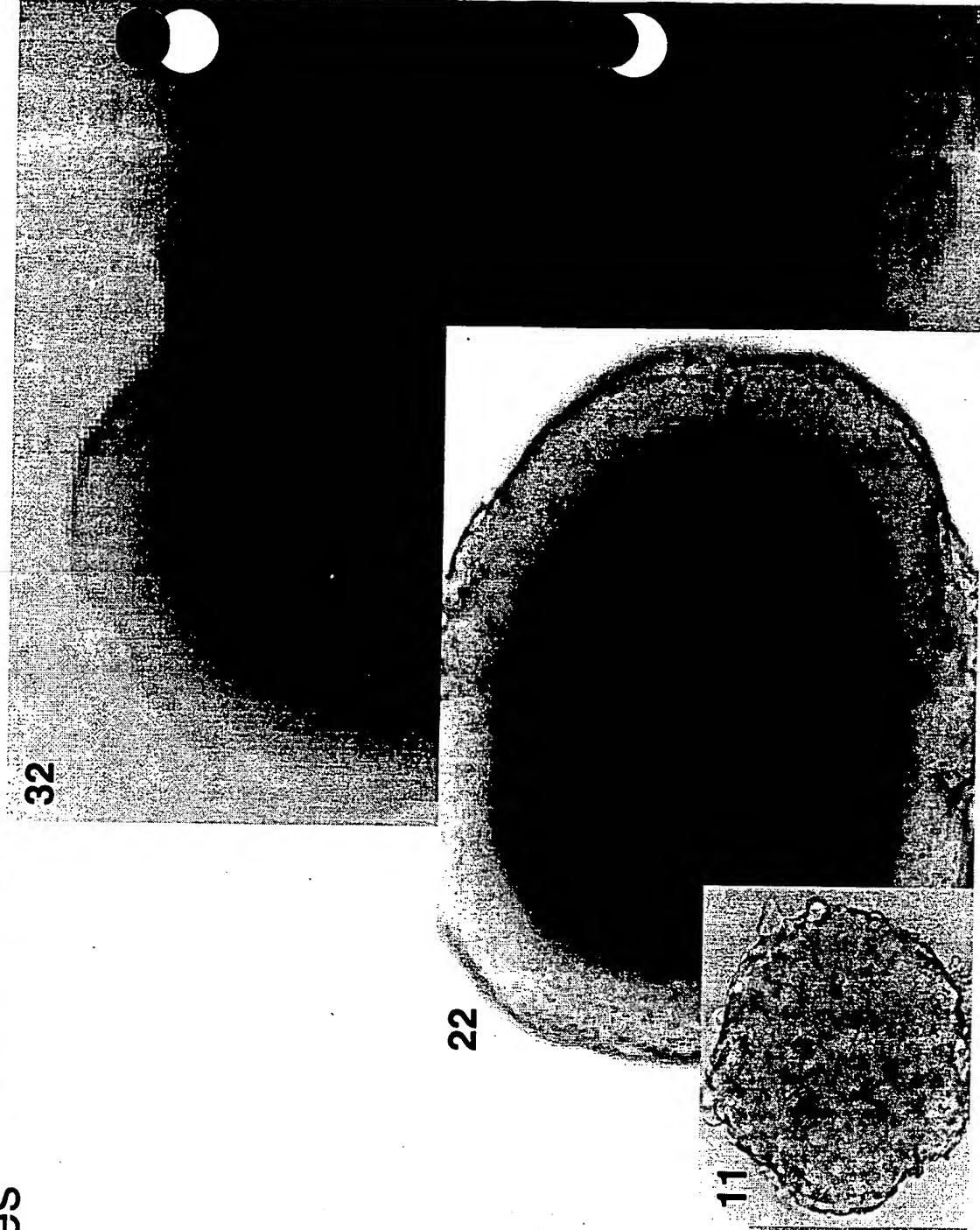
HuM195 (control)



J591 (specific)



Light microscope images of LNCaP-LN3 spheroids incubated 18 h with 25 $\mu\text{Ci/ml}$ ^{213}Bi -J591.

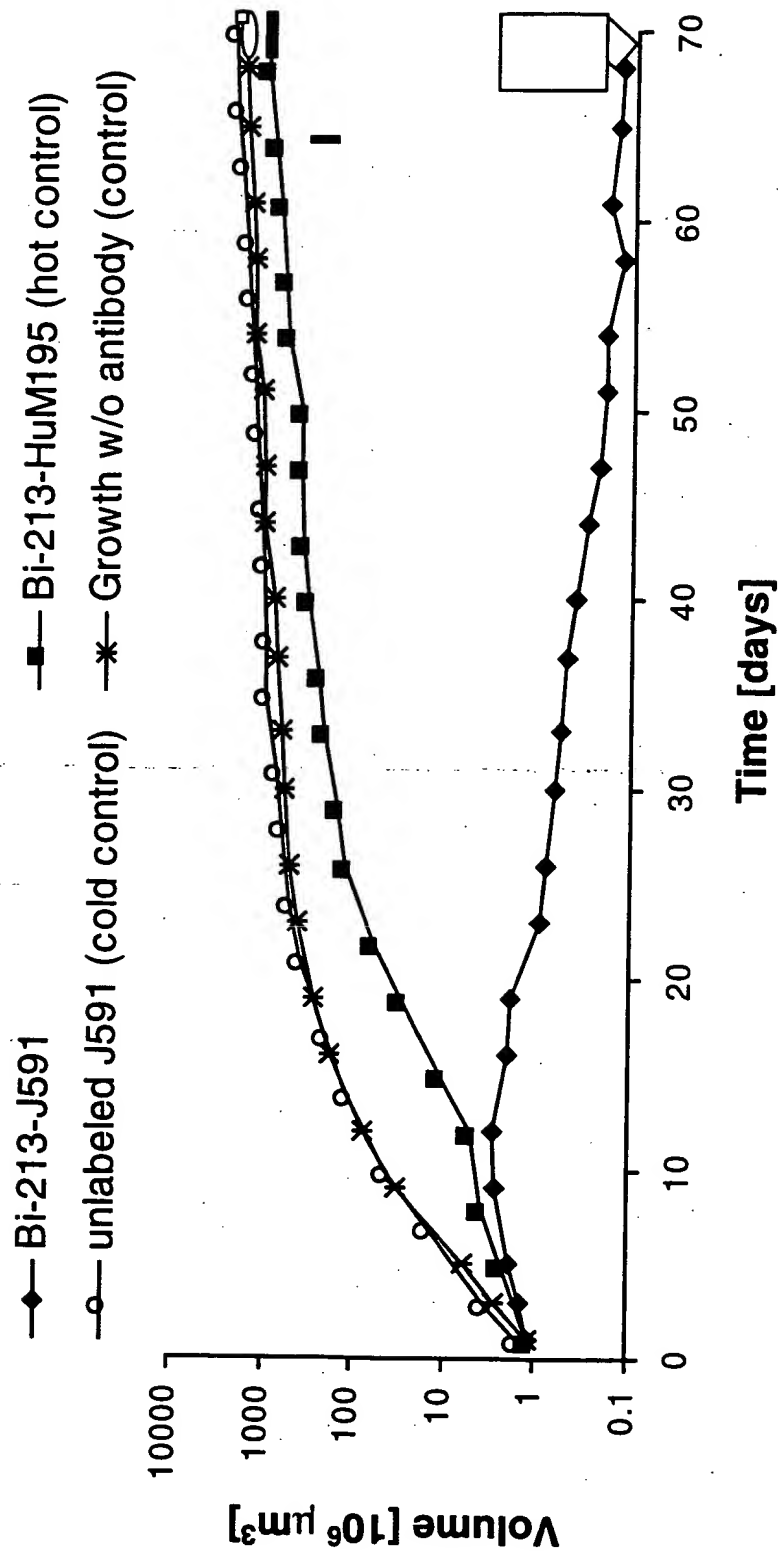


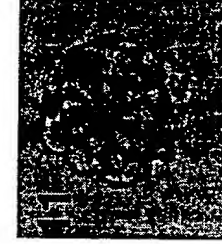
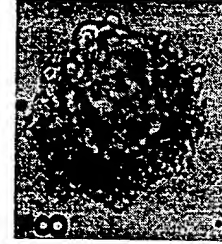
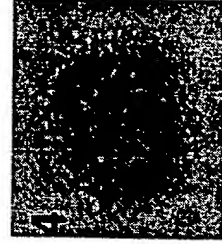
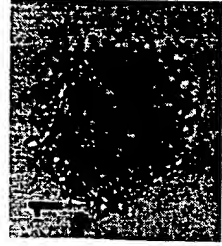
Hot control:
Light microscope images of LNCaP-LN3 spheroids incubated 18 h with 25 $\mu\text{Ci/ml}$ ^{213}Bi -HuM195.



Growth Delay

Median spheroid volume post incubation with 25 $\mu\text{Ci/ml}$ ^{213}Bi .
Diameter on day 0 was approximately 130 μm .





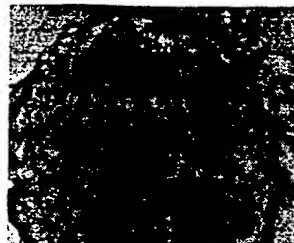
Spheroid 1

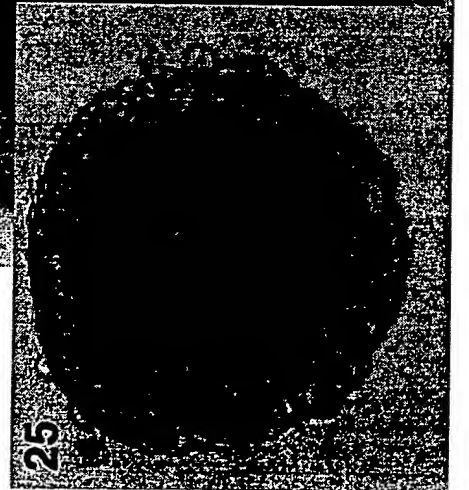
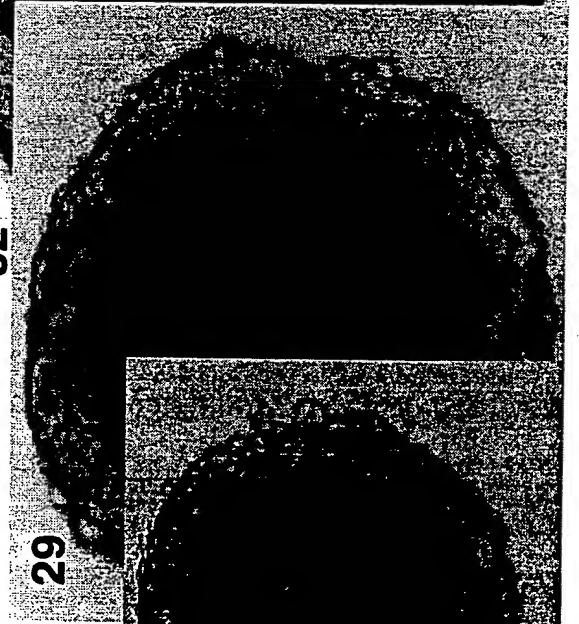
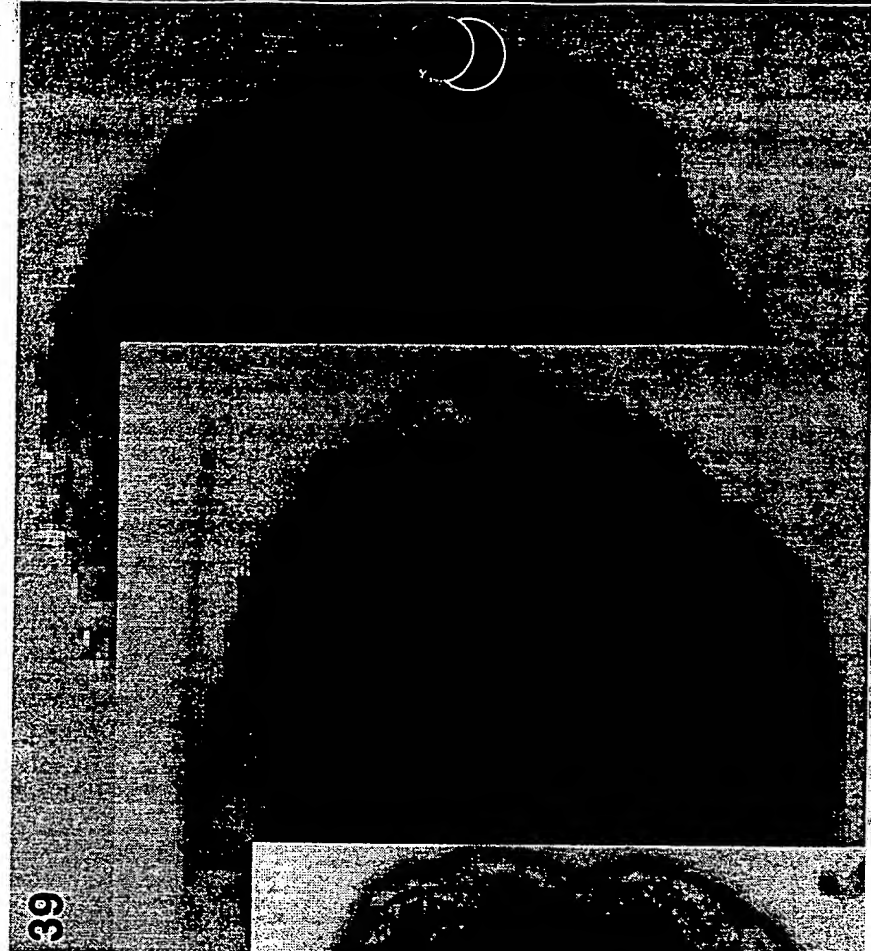
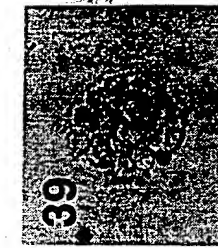
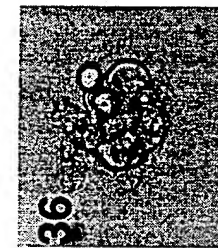
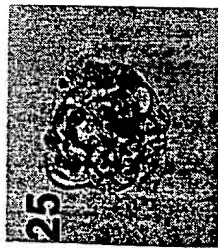
Light microscope images of LNCaP-LN3 spheroids incubated 18 h with 25 $\mu\text{Ci/ml}$ ^{213}Bi -J591.

The top and bottom panels show examples of spheroid break-up (top) and growth delay (bottom).

A prolonged growth delay relative to hot controls was seen in all treated spheroids.

Spheroid 2





The LNCaP spheroid model...

represents a well characterized model for prostate cancer.

is well suited for studies of the efficacy of alpha-particles since alphas have short range.

is relevant for antibody penetration studies and to investigate targeting of micrometastatic disease.

is an experimental analog which will help develop mathematical models to assist the development of optimal clinical therapy. This will be important for treatment of micrometastases where targeting and response cannot be easily monitored in patients.

(247 μ Ci, 27.3 μ g Ab, 2ml)

Graph 5. ^{90}Y -HuM195, 5 h, without Dexamethasone

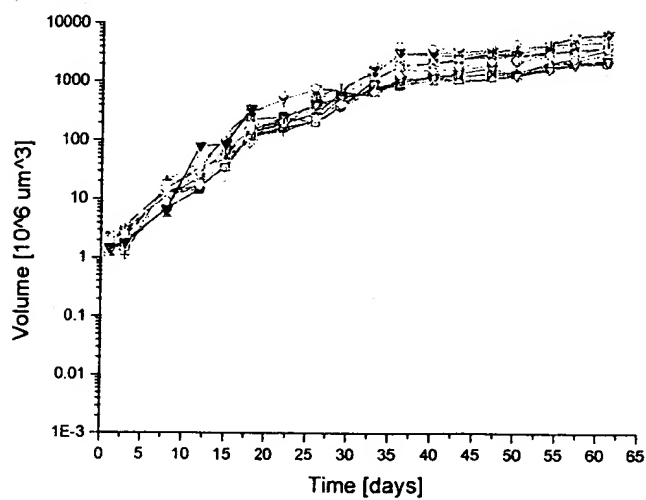
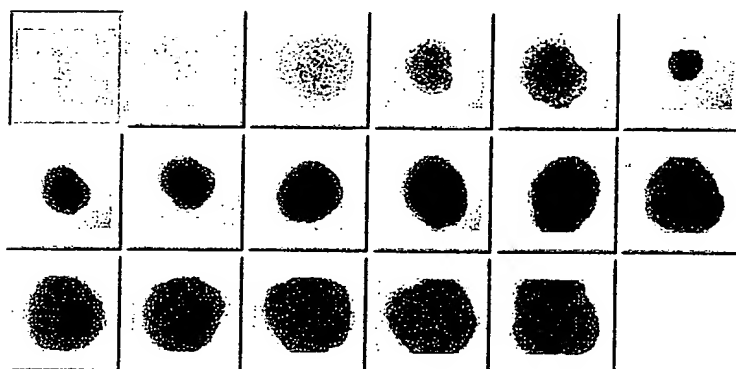


Figure 5. ^{90}Y -HuM195, 5 h, without Dexamethasone*



Graph 6. ^{90}Y -HuM195, 5 h, with Dexamethasone

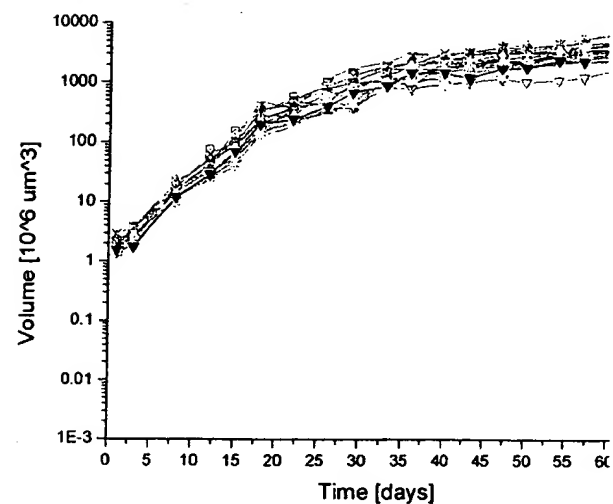
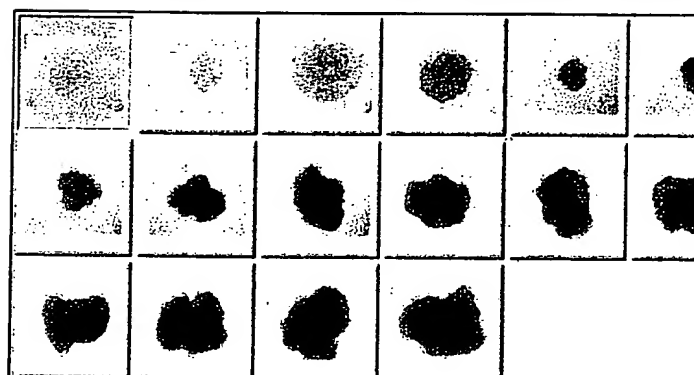


Figure 6. ^{90}Y -HuM195, 5 h, with Dexamethasone*



(247 μ Ci, 27.3 μ g Ab, 2ml)

Graph 7. ^{90}Y -HuM195, 19 h, without Dexamethasone

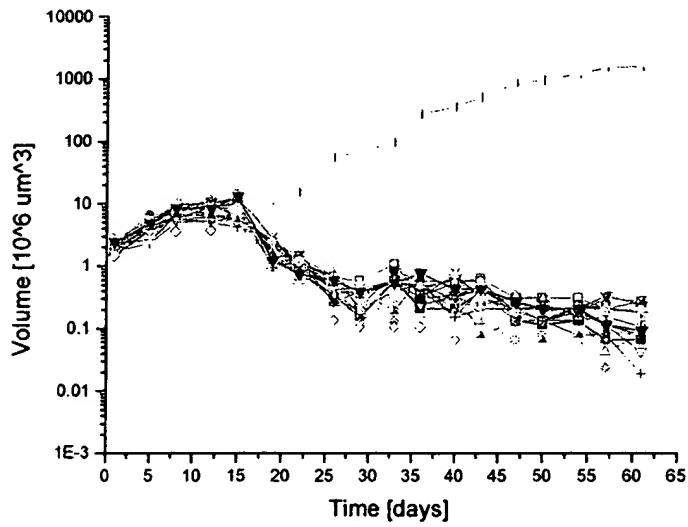
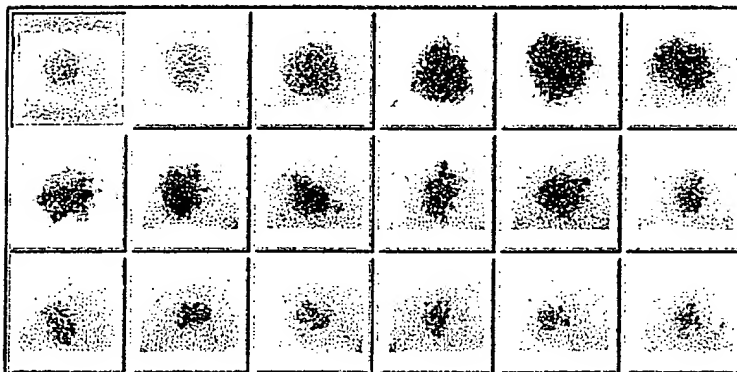


Figure 7. ^{90}Y -HuM195, 19 h, without Dexamethasone*



Graph 8. ^{90}Y -HuM195, 19 h, with Dexamethasone

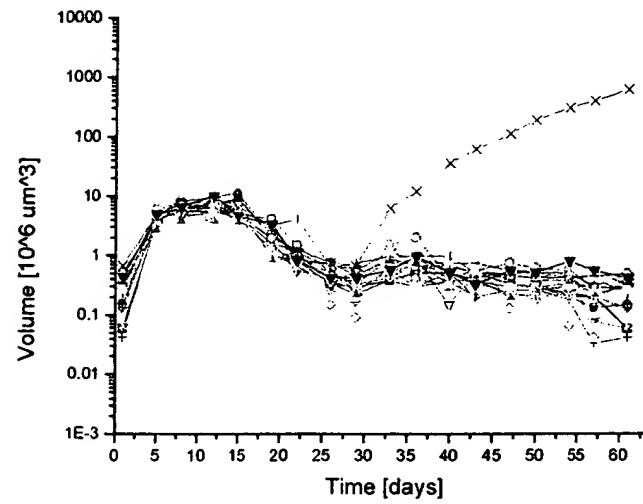
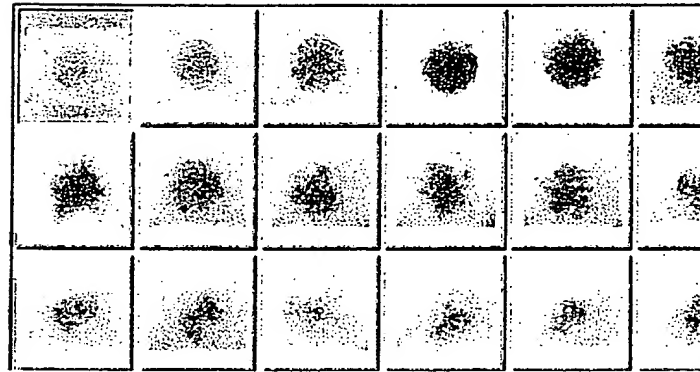


Figure 8. ^{90}Y -HuM195, 19 h, with Dexamethasone



Graph 9. External Beam, 6 Gy, without Dexamethasone

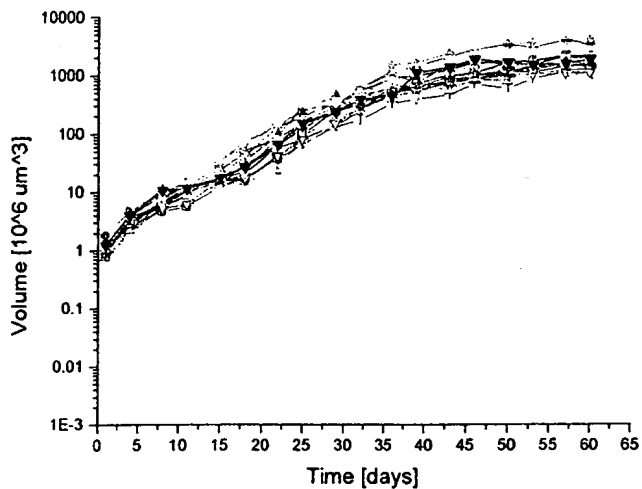
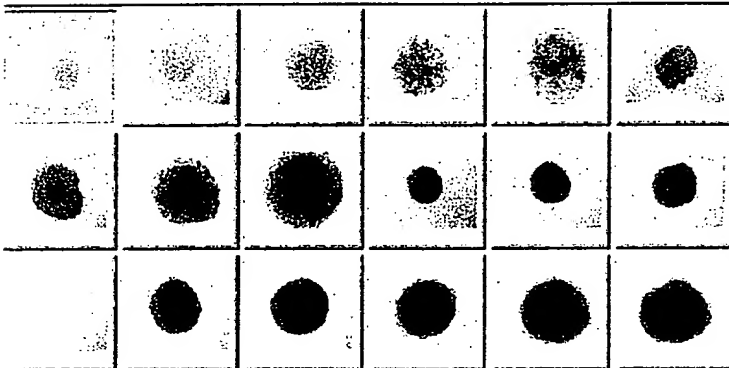


Figure 9. External Beam, 6 Gy, without Dexamethasone*



Graph 10. External Beam, 6 Gy, with Dexamethasone

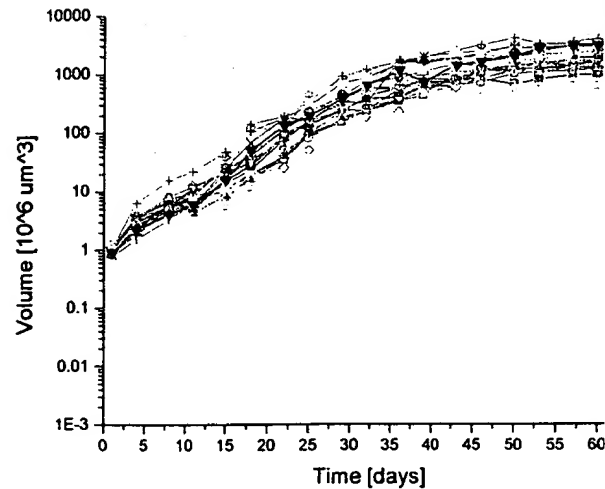
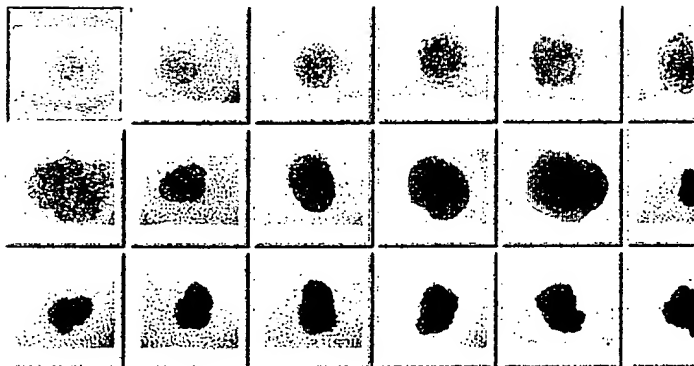


Figure 10. External Beam, 6 Gy, with Dexamethas



Graph 11. External Beam, 12 Gy, without Dexamethasone

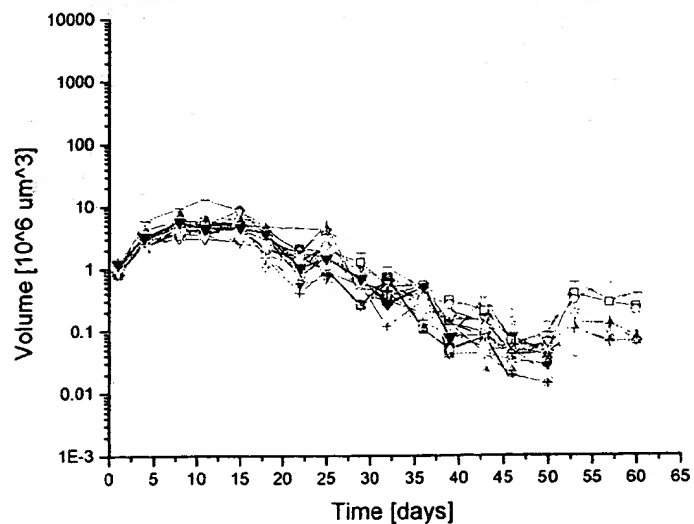
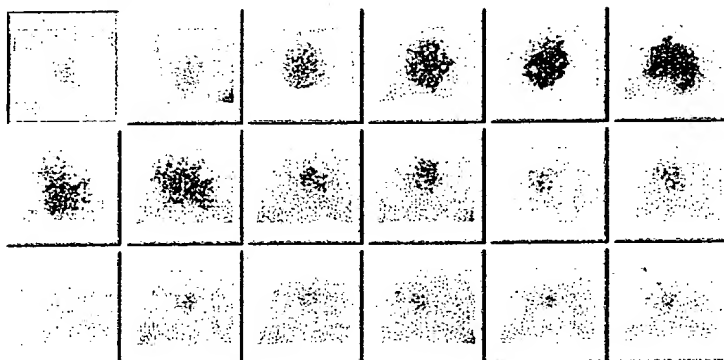


Figure 11. External Beam, 12 Gy, without Dexamethasone*



Graph 12. External Beam, 12 Gy, with Dexametha

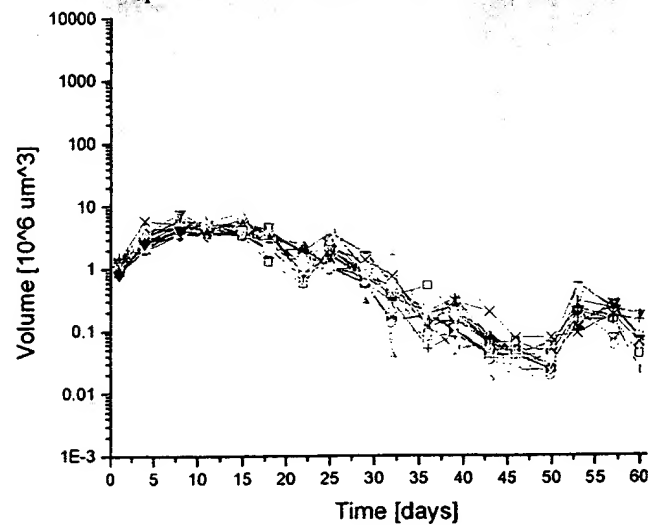
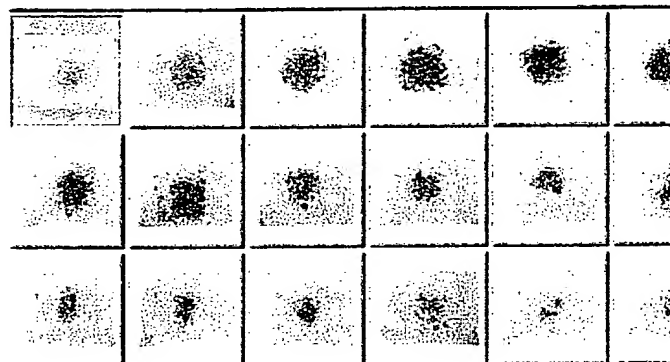


Figure 12. External Beam, 12 Gy, with Dexametha



(247 μCi , 27.3 μg Ab, 2ml)

Graph 13. ^{90}Y -J591, 5 h, without Dexamethasone

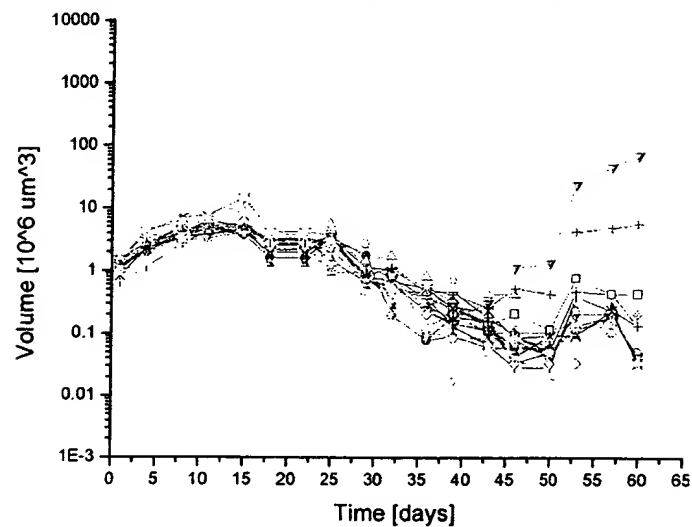
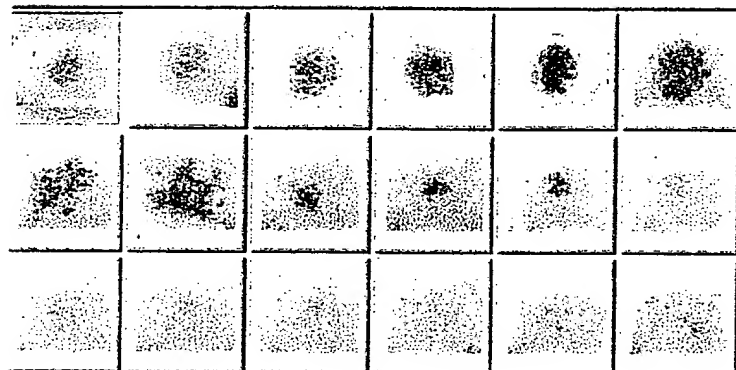


Figure 13. ^{90}Y -J591, 5 h, without Dexamethasone*



Graph 14. ^{90}Y -J591, 5 h, with Dexamethasone

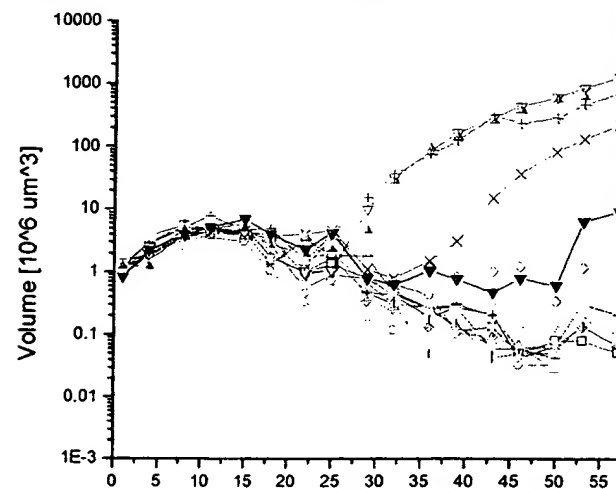
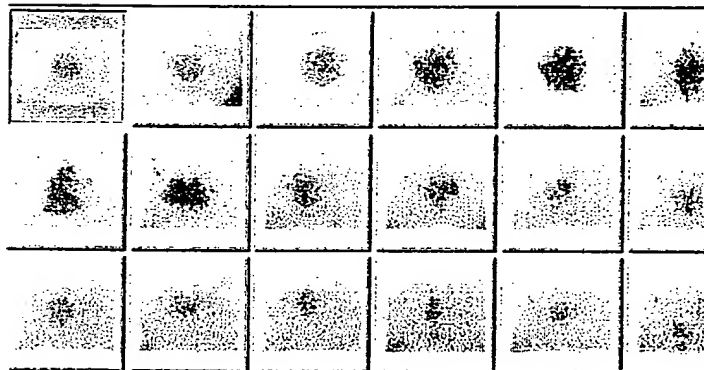


Figure 14. ^{90}Y -J591, 5 h, with Dexamethasone
(Days 1 to 32)



(247 μ Ci, 27.3 μ g Ab, 2ml)

Graph 15. ^{90}Y -J591, 19 h, without Dexamethasone

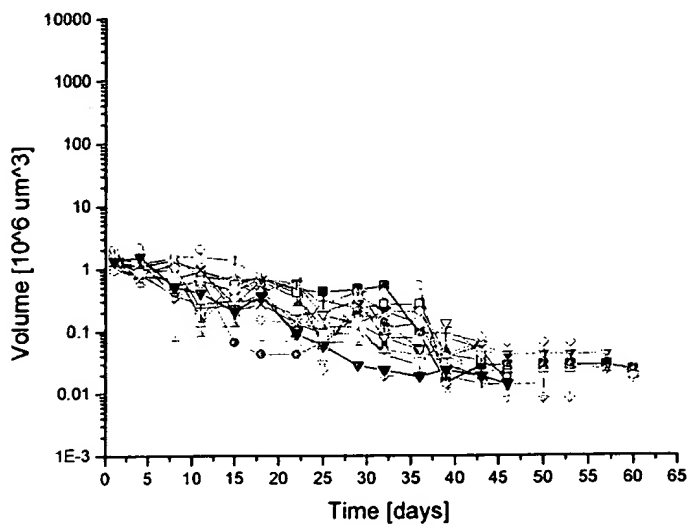


Figure 15. ^{90}Y -J591, 19 h, without Dexamethasone*

Graph 16. ^{90}Y -J591, 19 h, with Dexamethasone

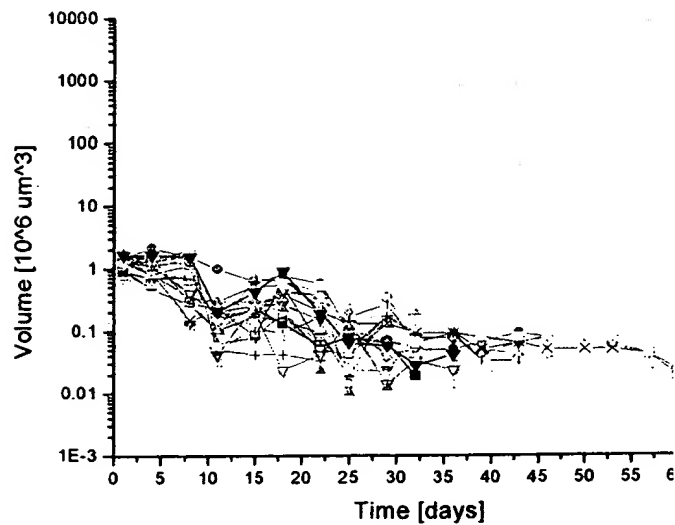


Figure 16. ^{90}Y -J591, 19 h with Dexamethasone (Days 1 to 32)

